Earth Syst. Dynam. Discuss., 6, 2101–2136, 2015
www.earth-syst-dynam-discuss.net/6/2101/2015/
doi:10.5194/esdd-6-2101-2015

Earth System Dynamics
Open Access
Discussions

Deforestation in Amazonia impacts riverine carbon dynamics

F. Langerwisch[1,2], A. Walz[3], A. Rammig[1,4], B. Tietjen[2,5], K. Thonicke[1,2], and W. Cramer[6]

[1]Earth System Analysis, Potsdam Institute for Climate Impact Research (PIK), P.O. Box 60 12 03, Telegraphenberg A62, 14412 Potsdam, Germany
[2]Berlin-Brandenburg Institute of Advanced Biodiversity Research (BBIB), 14195 Berlin, Germany
[3]Institute of Earth and Environmental Science, University of Potsdam, Karl-Liebknecht-Str. 24–25, 14476 Potsdam-Golm, Germany
[4]TUM School of Life Sciences Weihenstephan, Land Surface–Atmosphere Interactions, Technische Universität München, Hans-Carl-von-Carlowitz-Platz 2, 85354 Freising, Germany
[5]Biodiversity and Ecological Modelling, Institute of Biology, Freie Universität Berlin, Altensteinstr. 6, 14195 Berlin, Germany
[6]Institut Méditerranéen de Biodiversité et d'Ecologie marine et continentale (IMBE), Aix Marseille Université, CNRS, IRD, Avignon Université, Technopôle Arbois-Méditerranée, Bât. Villemin – BP 80, 13545 Aix-en-Provence CEDEX 04, France

Received: 30 September 2015 – Accepted: 8 October 2015 – Published: 22 October 2015

Correspondence to: F. Langerwisch (langerwisch@pik-potsdam.de)

Published by Copernicus Publications on behalf of the European Geosciences Union.

ESDD
6, 2101–2136, 2015

Abstract

Fluxes of organic and inorganic carbon within the Amazon basin are considerably controlled by annual flooding, which triggers the export of terrigenous organic material to the river and ultimately to the Atlantic Ocean. The amount of carbon imported to the river and the further conversion, transport and export of it, depend on terrestrial productivity and discharge, as well as temperature and atmospheric CO_2. Both terrestrial productivity and discharge are influenced by climate and land use change. To assess the impact of these changes on the riverine carbon dynamics, the coupled model system of LPJmL and RivCM (Langerwisch et al., 2015) has been used. Vegetation dynamics (in LPJmL) as well as export and conversion of terrigenous carbon to and within the river (RivCM) are included. The model system has been applied for the years 1901 to 2099 under two deforestation scenarios and with climate forcing of three SRES emission scenarios, each for five climate models. The results suggest that, following deforestation, riverine particulate and dissolved organic carbon will strongly decrease by up to 90 % until the end of the current century. In parallel, discharge increases, leading to roughly unchanged net carbon transport during the first decades of the century, as long as a sufficient area is still forested. During the following decades the amount of transported carbon will decrease drastically. In contrast to the riverine organic carbon, the amount of riverine inorganic carbon is only determined by climate change forcing, namely increased temperature and atmospheric CO_2 concentration. Mainly due to the higher atmospheric CO_2 it leads to an increase in riverine inorganic carbon by up to 20 % (SRES A2). The changes in riverine carbon fluxes have direct effects on the export of carbon, either to the atmosphere via outgassing, or to the Atlantic Ocean via discharge. Basin-wide the outgassed carbon will increase slightly, but can be regionally reduced by up to 60 % due to deforestation. The discharge of organic carbon to the ocean will be reduced by about 40 % under the most severe deforestation and climate change scenario. The changes would have local and regional consequences

ESDD
6, 2101–2136, 2015

Deforestation in Amazonia impacts riverine carbon dynamics

F. Langerwisch et al.

on the carbon balance and habitat characteristics in the Amazon basin itself but also in the adjacent Atlantic Ocean.

1 Introduction

The Amazon basin, defined as the drainage area of the Amazon River, covers approximately six million square kilometres, and more than 70 % of it is still covered with intact rainforest (Nobre, 2014). The amount of carbon in biomass in Amazonian rainforest is estimated to be $93 \pm 23 \times 10^{15}$ g C (Malhi et al., 2006). This biomass is stored in a wide range of diverse habitats, including tropical rainforest and savannahs, as well as numerous aquatic habitats, like lakes and wetlands (Goulding et al., 2003; Eva et al., 2004; Keller et al., 2009; Junk, 1997). The large diversity in habitats, partly already founded in the geologic formation of Amazonia, leads to a high diversity of animal and plant species (Hoorn et al., 2010), making the Amazon rainforest one of Earth's greatest collections of biodiversity. The Amazon River, which floods annually large parts of the forest, plays an important role in supporting the diversity of Amazonian ecosystems. The flooding is most decisive for the coupling of terrestrial and aquatic processes by transporting organic material from the terrestrial ecosystems to the river (Hedges et al., 2000). The input of terrigenous organic material (Melack and Forsberg, 2001; Waterloo et al., 2006), acts, for instance, as fertilizer and food source (Anderson et al., 2011; Horn et al., 2011), and is a modifier of habitats and interacting local carbon cycles (Hedges et al., 2000; Irmler, 1982; Johnson et al., 2006; McClain and Elsenbeer, 2001). On a larger scale, the release of carbon from the river into the atmosphere, and its export to the ocean are most relevant factors when it comes to assessing the effects of Amazon ecosystem on climate change. It is estimated that the large scale outgassing of carbon from the Amazon River plays an important role in assessing the future role of the Amazon basin as a carbon sink or source to the atmosphere. Approximately 470×10^{12} g C yr^{-1} is exported to the atmosphere as CO_2 (Richey et al., 2002),

ESDD
6, 2101–2136, 2015

in comparison with about 32.7×10^{12} g C yr^{-1} of total organic carbon (TOC) is exported to the Atlantic Ocean (Moreira-Turcq et al., 2003).

Deforestation continues to be the largest threat to Amazonia. The transformation of tropical rainforest to cropland and pasture impacts ecosystem stability profoundly due to altered climate regulation and species richness (Foley et al., 2007; Lawrence and Vandecar, 2014; Malhi et al., 2008; Spracklen et al., 2012). Until the year 2012 approximately 20 % of the original forest of the Brazilian part of the Amazon basin has been deforested, corresponding to an area of about 750 000 km^2 (Godar et al., 2014; INPE, 2013). This deforestation was mainly driven by the land expansion for soybean and cattle production and the expansion of the road network (Malhi et al., 2008; Soares-Filho et al., 2006). Together with climate change effects and forest burning, land cover change is predicted to release carbon at rates of 0.5–1.0 $\times 10^{15}$ g C yr^{-1} from this area (Potter et al., 2009). Furthermore, the annual CO_2 efflux from pasture soils exceeds that of mature and secondary forest (Salimon et al., 2004). The effects of deforestation on terrestrial carbon storage and fluxes persist several decades after logging because the forest needs about 25 years to recover approximately 70 % of their original biomass, and at least another 50 years for the remaining 30 % after abandonment of agriculture (Brown and Lugo, 1990; Houghton et al., 2000).

Due to the extraction of wood, deforestation leads to immediate changes in the terrestrial organic carbon pools that fuel riverine respiration (Mayorga et al., 2005), increase in velocity and amount of runoff, and discharge (Foley et al., 2002; Costa et al., 2003). Additionally, changes in precipitation caused by climate change alter inundation patterns (Langerwisch et al., 2013) like temporal shifts in high and low water months and changes of inundated area. The combined effects of climate change and deforestation has the potential to alter the exported terrigenous carbon fluxes as well as the amount of carbon that is exported to either the atmosphere or the ocean tremendously. The local import of carbon to the river can act as nutrient supply and therefore alters the habitat for plants and animals inhabiting the river, while the regional export of car-

ESDD
6, 2101–2136, 2015

bon form the entire Amazon basin alters the amount of carbon stored and therewith the carbon-sink potential of Amazonia (Hamilton, 2010).

The aim of our study is to elaborate on these combined effects of climate change and deforestation on the riverine carbon fluxes, on the export of organic material into the Atlantic Ocean and on the outgassing of riverine carbon to the atmosphere.

To address these issues basin-wide data are needed, which not only describe the current situation but also assess future developments. On-site measurements are limited to some certain point in time and/or space. To partly overcome these limitations we make use of the well-established dynamic global vegetation model LPJmL together with the riverine carbon model RivCM. While LPJmL (Bondeau et al., 2007; Gerten et al., 2004; Rost et al., 2008; Sitch et al., 2003) provides plausible estimates for the carbon and water pools and fluxes within the coupled soil-vegetation system, RivCM (Langerwisch et al., 2015) focuses on the export, conversion and transport of terrestrial fixed carbon in the river and to the atmosphere and ocean. To investigate the effects of climate change and deforestation on the riverine carbon the coupled model was forced by several climate change and deforestation scenarios that cover a wide range of uncertainties. We estimated temporal and spatial changes in three riverine carbon pools as well as changes in the export of carbon to the atmosphere and the ocean.

2 Methods

The impacts of climate change and deforestation on riverine carbon pools and fluxes in the Amazonian watershed are assessed by the model RivCM (Langerwisch et al., 2015) for a range of scenarios. RivCM is a grid-based model that assesses the transport and export of carbon at monthly time steps and is driven climate data and terrestrial carbon pools. Climate inputs are taken from different global climate model simulations driven by three SRES scenarios (Nakićenović et al., 2000). Terrestrial carbon inputs are estimated by the process-based dynamic global vegetation and hydrology model LPJmL (Bondeau et al., 2007; Gerten et al., 2004; Rost et al., 2008; Sitch et al.,

ESDD
6, 2101–2136, 2015

2003). To estimate soil and vegetation carbon, LPJmL uses the above mentioned climate data and a set of deforestation scenarios from a regional projections by SimAmazonia (Soares-Filho et al., 2006). An overview of the interconnection between the two models and the scenarios is given in Fig. 1.

2.1 Model descriptions

2.1.1 LPJmL – a dynamic global vegetation and hydrology model

The process-based global vegetation and hydrology model LPJmL (Bondeau et al., 2007; Gerten et al., 2004; Rost et al., 2008; Sitch et al., 2003) calculates carbon and corresponding water fluxes globally on a spatial resolution of $0.5^{\circ} \times 0.5^{\circ}$ (lat/lon) in daily time steps. For calculating the main processes, controlling the dynamics of potential natural vegetation and thus carbon pools for vegetation, litter and soil, LPJmL uses climate data (temperature, precipitation, and cloud cover), atmospheric CO_2 concentration, and soil type as input. The main processes are photosynthesis, which is modelled according to Farquhar et al. (1980) and Collatz et al. (1992), auto- and heterotrophic respiration, establishment, mortality, and phenology. The simulated water fluxes include evaporation, soil moisture, snowmelt, runoff, discharge, interception, and transpiration, which are directly linked to abiotic and biotic properties. In each grid cell LPJmL calculates the performance of nine plant functional types, which represent an assortment of species classified as being functionally similar. In the Amazon basin primarily three of these types are present, namely tropical evergreen and deciduous trees and C4 grasses. In addition to the potential natural vegetation LPJmL can simulate the dynamics of 16 user-defined crops and pasture on area that is not covered by natural vegetation. In analogy to natural vegetation, LPJmL evaluates carbon storage in vegetation, litter and soil as well as water fluxes for these areas.

LPJmL has been shown to reproduce current patterns of biomass production (Cramer et al., 2001; Sitch et al., 2003), carbon emission through fire (Thonicke et al., 2010), also including managed land (Bondeau et al., 2007; Fader et al., 2010; Rost

ESDD
6, 2101–2136, 2015

et al., 2008), and water dynamics (Biemans et al., 2009; Gerten et al., 2004, 2008; Gordon et al., 2004; Wagner et al., 2003). The simulated patterns in water fluxes, like evapotranspiration, runoff and soil moisture, are comparable to stand-alone global hydrological models (Biemans et al., 2009; Gerten et al., 2004; Wagner et al., 2003).

2.1.2 RivCM – a riverine carbon model

RivCM is a process-based model that calculates four major ecological processes related to the carbon budget of the Amazon River (Fig. 1b). These processes include (1) mobilization, (2) decomposition and (3) respiration within the river, and (4) outgassing of CO_2 to the atmosphere (Langerwisch et al., 2015). During mobilization parts of terrigenous litter and soil carbon, as it is provided by LPJmL, is imported to the river, depending on inundated area. The further processing of the terrigenous carbon in the river happens during its decomposition, which represents the manual breakup, and its respiration, representing the biochemical breakup. Finally the CO_2 that is produced during respiration can outgas if the saturation concentration is exceeded (Langerwisch et al., 2015). These four processes directly control the most relevant riverine carbon pools, namely particulate organic carbon (POC), dissolved organic carbon (DOC), and inorganic carbon (IC), as well as outgassed atmospheric carbon (representing CO_2), and exported riverine carbon to the ocean (either as POC, DOC, or IC).

The model is coupled to LPJmL by using the calculated monthly litter and soil carbon and water amounts as inputs. It operates at the spatial resolution of $0.5^\circ \times 0.5^\circ$ (lat/lon) and on monthly time steps. The ability of the coupled model LPJmL–RivCM to reproduce current conditions in riverine carbon concentration and export to either the atmosphere or the ocean has been shown and discussed by Langerwisch et al. (2015). Here, we use the coupled model to assess the combined impacts of climate change and deforestation.

ESDD
6, 2101–2136, 2015

2.2 Model simulation

All transient LPJmL runs were preceded by a 1000 year spin-up during which the pre-industrial CO_2 level of 280 ppm and the climate of the years 1901–1930 have been repeated to obtain equilibria for vegetation, carbon, and water pools. All transient runs of the coupled model LPJmL–RivCM have been preceded by a 90 years-spinup during which the climate and CO_2 levels of 1901–1930 have been repeated to obtain equilibria for riverine carbon pools.

LPJmL–RivCM was run on a $0.5^{\circ} \times 0.5^{\circ}$ (lat/lon) spatial resolution for the years 1901 to 2099. For the estimation of the impact of projected climate change (CC) and deforestation (Defor), simulations have been conducted driven by five General Circulation Models (GCMs), each calculated for three SRES emission scenarios, and three LUC scenarios.

Climate change and deforestation data sets

To assess the effect of future climate change, projections of five GCMs (see also Jupp et al., 2010; Randall et al., 2007), using three SRES scenarios (A1B, A2, B1) (Nakićenović et al., 2000) have been applied (Fig. 1a). The GCMs, namely MIUB-ECHO-G, MPI-ECHAM5, MRI-CGCM2.3.2a, NCAR-CCSM3.0, UKMO-HadCM3, cover a wide range in terms of temperature and precipitation and have therefore been chosen to account for uncertainty in climate projections. The emission scenario SRES A1B describes a development of very rapid economic growth with convergence among regions, and a balanced future energy source between fossil and non-fossil. SRES A2 describes a development of a very heterogeneous world with slow economic growth. And SRES B1 describes a development of converging world similar to A1B but with more emphasis on service and information economy.

To estimate the additional effects of deforestation on riverine carbon pools and fluxes three land use scenarios were applied: two scenarios directly relate to different intensity of deforestation, and one represents a reference scenario with complete coverage by natural vegetation (NatVeg scenario, hereafter). The two deforestation scenarios are based on the SimAmazonia projections (Soares-Filho et al., 2006). The authors estimate the development of deforestation in the Amazon basin until 2050 based on historical trends and projected developments. In the business-as-usual scenario (BAU) they assume that recent deforestation trends continue, the number of paved highways increases, and new protected areas are not established. In contrast, deforestation is more efficiently controlled in the governance scenario (GOV). For this scenario the authors assume that the Brazilian environmental legislation is implemented across the Amazon basin and the size of the area under the Protected Areas Program increases. The SimAmazonia scenarios cover the years from 2001 to 2050. The period between 2051 and 2099 was further included into our study to show the long term effects of deforestation, while further deforestation is neglected over this period. In addition deforestation rates preceding the deforestation scenarios were derived from extrapolating the data into the past. For that, the mean annual rate of deforestation was calculated for the reference period of 2001 to 2005 (Eq. 1) and this rate was applied to calculate the fraction of deforested area F_t for the years 1901 to 2000 for each cell (Eq. 2).

$$r = \left(\sum_{t_{\text{ref}}=2001}^{2005} \frac{F_{t_{\text{ref}}}}{F_{t_{\text{ref}}+1}} \right) \times \frac{1}{2006 - 2001} \quad (1)$$

$$F_t = F_{2001} \times r^{2001-t} \quad (2)$$

Figure 2 shows an overview of deforested cell fraction in 2050 in the BAU scenario. To evaluated special differences in the basin we defined three sub-regions (see Table 1). Three regions were selected for further detailed analysis (Fig. 2). R1 is located in the Western basin with projected increase in inundation length and inundated area (Langerwisch et al., 2013) combined with low land use intensity. R2 is a region covering the Amazon main stem with intermediate changes in inundation (Langerwisch et al., 2013) and intermediate land use intensity. And R3 is a region with projected decrease in duration of inundation and inundated area (Langerwisch et al., 2013) combined with

ESDD
6, 2101–2136, 2015

high land use intensity. In the deforestation scenarios we assume that on 15 % of the deforested area soy bean is grown and 85 % of the area is used as pasture for beef production (Costa et al., 2007).

2.3 Analysis of simulation results

The net effect of deforestation (E_{Defor}) is estimated by calculating the differences between future carbon amounts (2070–2099) produced in the deforestation scenarios (GOV or BAU) and future carbon amounts produced in the potential natural vegetation scenario (NatVeg), where no deforestation is assumed. The combined effect of climate change and deforestation (E_{CCDefor}) is estimated by calculating the differences between future carbon amounts produced in the deforestation scenarios and reference carbon amounts (1971–2000) produced in the NatVeg scenario. Carbon can occur in the river either in an organic or inorganic form. Therefore the following four different carbon pools have been analysed: the riverine particulate organic carbon (POC) and dissolved organic carbon (DOC), as well as the riverine inorganic carbon pool (IC) and outgassed carbon. The relative changes in POC and DOC show similar patterns (see Fig. S1 in the Supplement), therefore exemplary POC is shown and discussed in detail.

2.3.1 Evaluation of potential future changes

Spatial effects of the two deforestation scenarios (GOV and BAU) on the different riverine carbon pools and fluxes have been estimated by calculating the common logarithm ($\log_{10}$) of the ratio of mean future (2070–2099) carbon amounts of the deforestation scenarios and mean future carbon amounts of the NatVeg scenario (E_{Defor}, Eq. 3) for each simulation run.

$$E_{\text{Defor}} = \log_{10} \frac{\sum_{t=2070}^{2099} C_{\text{Defor}_t}}{\sum_{t=2070}^{2099} C_{\text{NatVeg}_t}} \quad (3)$$

Discussion Paper | Discussion Paper | Discussion Paper | Discussion Paper |

ESDD

6, 2101–2136, 2015

Deforestation in Amazonia impacts riverine carbon dynamics

F. Langerwisch et al.

To estimate changes caused by the combination of climate change and deforestation E_{CCDefor} compares future carbon pools in the deforestation scenarios to carbon pools during the reference period (1971–2000) in the NatVeg scenario (Eq. 4).

$$E_{\mathrm{CCDefor}} = \log_{10} \frac{\sum_{t1=2070}^{2099} C_{\mathrm{Defor}_{t1}}}{\sum_{t2=1971}^{2000} C_{\mathrm{NatVeg}_{t2}}} \quad (4)$$

Each simulation run combines deforestation and emission scenarios and aggregates the outputs for all five climate model inputs used. To identify areas where the differences between values in the reference period and future values are significant (p value < 0.05), the Wilcoxon Rank Sum Test for not-normally distributed datasets (Bauer, 1972) has been applied for each cell.

Additionally to the spatial assessment, time series were deduced based on mean values over the entire basin and each of the three exemplary regions R1, R2 and R3. These means of the carbon pools were calculated for every year during the simulation period. Changes have been expressed as the five-year-running-mean of the quotient of annual future carbon amounts in the deforestation and in the NatVeg scenarios. These analyses have been conducted both for the whole Amazon basin and for three selected sub-regions.

2.3.2 Estimating the dominant driver for changes

We estimated which factor is causing the observed changes the most. To estimate the contribution of either climate change (D_{CC}, Eq. 5) or deforestation (D_{Defor}, Eq. 6), reference carbon amounts of the NatVeg scenario have been compared to future amounts of the NatVeg scenario (D_{CC}), and future carbon amounts of the NatVeg scenario have been compared to future amounts of the deforestation scenarios (D_{Defor}).

ESDD
6, 2101–2136, 2015

Title Page
Abstract | Introduction
Conclusions | References
Tables | Figures
Back | Close
Full Screen / Esc
Printer-friendly Version
Interactive Discussion

$$D_{\mathrm{CC}} = \left| \log_{10} \frac{\sum_{t1=2070}^{2099} C_{\mathrm{NatVeg}_{t1}}}{\sum_{t2=1971}^{2000} C_{\mathrm{NatVeg}_{t2}}} \right| \tag{5}$$

$$D_{\mathrm{Defor}} = |E_{\mathrm{Defor}}| \tag{6}$$

We define a cell as dominated by climate change effects, if $D_{\mathrm{CC}} > D_{\mathrm{Defor}}$ and dominated by deforestation effects if $D_{\mathrm{CC}} < D_{\mathrm{Defor}}$. The impact values D_{CC} and D_{Defor} (median$_{\mathrm{POC}}$ = 0.9695, median$_{\mathrm{IC}}$ = 1.0106, and median$_{\mathrm{outgassedC}}$ = 0.9982) have been rounded to the second decimal place. If both values are equal, the two effects balance each other.

3 Results

3.1 Changes caused by deforestation

Deforestation leads to a decrease in riverine particulate and dissolved organic carbon (POC and DOC). Figure 3a and b shows that the decrease is more intense under the BAU than under the GOV scenario (for DOC see Fig. S1a and b). In some highly deforested sites the POC amount is only 10 % (indicated by $10^{-1.0}$ in the maps) of the amount under no deforestation (indicated by E_{Defor}). This pattern is robust between the model realizations with a high agreement of the results amongst the five climate models. Compared to the deforestation scenarios the differences between the three emission scenarios (A1B, A2, and B1) are very small, i.e. even under the moderate emission scenario B1 the decrease in POC can be drastic. Despite the overall decrease there are few areas where POC increases (up to 3fold, $10^{0.5}$), especially in mountain regions (e.g. Andes and Guiana Shield). DOC and POC follow the same spatial and temporal patterns in change (see Fig. S1) therefore only one of the carbon pools, namely POC, is shown and discussed in detail. Although POC and DOC respond similar in relative terms, the absolute amounts are approximately twice as high for DOC compared to POC (Table 2). The mean basin-wide loss in POC ranges between $0.13 \times 10^{12}\,\mathrm{g\,yr^{-1}}$ (A2) and 0.24 (A1B) $\times 10^{12}\,\mathrm{g\,yr^{-1}}$ (A1B) in the GOV scenario, and between $0.37 \times 10^{12}\,\mathrm{g\,yr^{-1}}$ (A2) and $0.48 \times 10^{12}\,\mathrm{g\,yr^{-1}}$ (A1B) in the BAU scenario. As with the relative changes the absolute differences show that compared to the deforestation scenarios the effect of the different emission scenarios on POC and DOC is small. The SRES A2 scenario causes the largest changes, further increasing the loss caused by land use change.

Changes in outgassed riverine carbon caused by deforestation (Fig. 3c and d) show a similar pattern as the changes in POC, with an even clearer effect of deforestation on a larger area. In both scenarios deforestation leads to a decrease in outgassed carbon to up to a tenth ($10^{-1.0}$) compared to the amount produced under the NatVeg scenario. The agreement between the five climate models is even larger than in POC. Some areas in the Andes and the Guiana Shield show an increase in outgassed carbon of up to a factor of 30 ($10^{1.5}$), but these areas are an exception. Like in POC the differences between the SRES scenarios are only minor. For the absolute values see Table 2.

For riverine inorganic carbon (IC) deforestation caused significant changes (E_{Defor}, p value < 0.05) only in small areas (Fig. 3e and f). In these regions, in the very South of the basin and in single spots in the North, i.e. in the headwaters of the watershed, IC increases by a factor of up to 1.2 ($10^{0.08}$). Besides these areas of increase, a slight decrease of about 5 % ($10^{-0.02}$) is simulated for the region along the main stem of the Amazon River, downstream of Manaus and along the Rio Madeira and the Rio Tapajós. In contrast to POC, the spatial pattern of change in IC does not obviously follow the deforestation patterns. Therefore, the differences between the two deforestation scenarios GOV and BAU scenarios are minor. Whereas POC, DOC, and outgassed carbon show a clear decrease due to deforestation, IC shows a nearly neutral response with maximal mean basin-wide gains (for absolute values see Table 2).

ESDD
6, 2101–2136, 2015

3.2 Changes caused by a combination of deforestation and climate change

Climate change and deforestation together will lead to large overall changes in the amount of riverine and exported carbon. Riverine POC and DOC amounts will decrease by about 19.8 and 22.2 %, respectively, and exported organic carbon will decrease by about 38.1 % (Fig. 4). In contrast riverine IC will increase by about 100 %, combined with a slight increase of outgassed carbon by about 2.7 % (Fig. 4). In detail, the basin-wide changes in the amount of POC (Figs. 5a, b and 6a) caused by deforestation and climate change range between a 2.5 fold increase ($10^{0.4}$) and a decrease to one tenth ($10^{-1.0}$). The increase is mainly caused by climate change (indicated by the green cell borders in Fig. 5), whereas the decrease is mainly caused by deforestation (red cell borders). The differences mainly induced by deforestation are larger in the BAU compared to the GOV scenario. In contrast, the differences caused by climate change show no large differences between the two deforestation scenarios. The differences between the emission scenarios are minor (see also Table 2). In some areas the dominance of forcing shifts from climate change dominance (D_{CC}) for the GOV scenario (green cell border) to deforestation dominance (D_{Defor}) for the BAU scenario (red cell border) due to the higher land use intensity as a result of deforestation (see also Table 3). While in the GOV scenario 20 % of all cells are dominated by deforestation impacts, this value increases for the BAU scenario to 30 %. During the first decades (2000–2030) basin-wide POC is partly larger in the deforestation scenarios than in the NatVeg scenario by up to 2 % in 2000 and about 1 % in 2020 (Fig. 6a). All climate models show reduced POC amounts in the deforestation scenarios compared to the NatVeg scenario after 2040. The POC amount in the GOV deforestation scenario decreases gradually until the decrease levels off in the late 2060s, i.e. ten years after the constant deforestation area is kept constant. In the BAU scenario, POC decreases strongly in the 2040 to 2060s leading to a loss of about 25 % compared to 10 % in the GOV scenario. The three sub-regions R1 to R3 show different patterns (Fig. 6a). While in region R1 the difference in the POC amounts between the GOV and the BAU

ESDD
6, 2101–2136, 2015

scenario is only small, reflecting the low deforestation in this region, the differences between the two deforestation scenarios are more explicit in regions R2 and especially in R3 (with the largest area deforested), where in addition model uncertainty is low. Starting in the 2050s, the variation between different emission scenarios and climate models increases. Alike the results of the impact of deforestation alone POC and DOC show a similar pattern. Therefore only results for POC are shown and explained in detail (see also Table 2).

The changes in outgassed carbon (Figs. 5c, d and 6b) are in the same range as changes in POC. The large-scale gain in outgassed carbon of about 20 % ($10^{0.5}$), especially in the North-Western basin, is driven by climate change (Fig. 5c and d). The deforestation induces a decrease to one tenth ($10^{-0.1}$) in areas with high fraction of deforested area, i.e. in the Eastern and South-Eastern basin. The effect of the two deforestation scenarios (GOV vs. BAU) is much larger than the effect of the different emission scenarios (see also Table 2). Temporarily the differences in the amount of outgassed carbon (Fig. 6b) show a strong deforestation-driven pattern as well. The outgassed carbon directly depends on the available POC, therefore the time series of both, POC and IC widely match. In the GOV scenario the basin-wide loss of outgassed carbon is about 16 % towards the end of the century. The results of the BAU scenario show an average loss of outgassed carbon of 28 %.

Changes in inorganic carbon (IC) are mainly caused by climate change for both deforestation scenarios and all emission scenarios (Figs. 5e, f and 6c, Tables 2 and 3). The IC amount significantly changes in about 50 % of the cells due to climate change and in no cell due to land use change. The magnitude of change varies between emission scenarios: the increase in IC is up to 4 fold ($10^{0.6}$) in the A2 scenario and up to 2.5 fold ($10^{0.4}$) in the B1 scenario (see Table 2). For both deforestation scenarios the gain of IC is dominant until 2050, while the basin-wide trend becomes unclear afterwards. However, sub-regions like R1 and R3 show a slight increase during the whole century (Fig. 6c).

ESDD
6, 2101–2136, 2015

4 Discussion

Deforestation is, besides climate change, the largest threat to Amazonia. It leads directly to a decrease in terrestrial biomass and an increase in CO_2 emissions (Potter et al., 2009) and has indirect effects on aquatic biomass, diversity of species and biotopes and the climate (Asner and Alencar, 2010; Bernardes et al., 2004; Costa et al., 2003).

4.1 Temporal trends in carbon pools

Our results show that deforestation leads to a basin-wide reduction in riverine particulate and dissolved organic carbon pools by the end of the century by about 10 to 25 % (Fig. 6). This reduction is particularly pronounced in areas of high deforestation intensity at the Arc of Deforestation, at the Rio Madeira and the last 500 km stretch of the Rio Amazon. In the first decades of the 21st century the differences in carbon amounts between the two land use intensities are only small (Fig. 6). During these decades in both scenarios a deforestation induced increase in discharge (as reported by Costa et al., 2003), is able to balance the decreasing amount of terrigenous organic matter which is the source of riverine organic matter. The differences in the organic carbon pools caused by deforestation become more obvious after the 2050s (Fig. 6), with larger carbon decrease in the more severe BAU scenario. After 2050 the deforested area remains constant and the variation within the results can be attributed to the climate models and emission scenarios.

4.2 Shortcomings of the deforestation scenarios and implementation of crops in LPJmL

The strong decrease of organic carbon is especially pronounced because we assume a complete removal of the natural vegetation carbon during deforestation. In reality, the complete conversion of the floodplain forests to cropland or pasture is not very

ESDD
6, 2101–2136, 2015

likely. In the more severe deforestation scenario (BAU) about 6 % of the area is deforested (Soares-Filho et al., 2006). In our scenarios this also includes areas which are temporarily flooded. This might sound unrealistic, since temporarily inundated areas cannot be easily converted to agricultural area or settlements. But on the other hand in Manaus, floodplains within a radius of about 500 km around the city have been extensively logged for construction purposes between 1960 and 1980 (Goulding et al., 2003).

In our study deforestation is simulated by partial or complete removal of vegetation carbon. This also reduces the litter and soil carbon through respiration over time in these areas, because these pools are not refilled by litter fall from the vegetation. Because the deforested cell fraction has been kept constant from 2050 to 2099 the results show how carbon pools stabilize after 2050.

4.3 Consequences of the changed riverine carbon pools

The reduction in the riverine organic carbon pools, which is caused by extensive deforestation, will have consequences for the floodplain and the river itself. Floodplains as well as riverine biotopes depend on the annually recurring input of organic material, either as food supply or fertilizer (Junk and Wantzen, 2004). The productivity of the floodplain forests is mainly driven by the input of nutrients which are basically sediments and organic material (Worbes, 1997). While the sediment input bringing new nutrients might increase due to increased discharge, the input of organic material from upstream areas will decrease, leading to a reduced productivity. This reduced productivity will certainly impact many animal species that rely on the food supplied by the trees, like fruits or leaves and in turn plant species composition on the local and regional scale (Junk and Wantzen, 2004; Worbes, 1997).

Additionally, deforestation will have secondary effects, including a reduction in evasion of CO_2 from the water (outgassed carbon). Lower terrestrial productivity after deforestation decreases the organic carbon material in the river and thus also the respiration to CO_2. This is opposed by the higher respiration rate as a result of increased

ESDD
6, 2101–2136, 2015

temperatures as part of the projected climate change. In addition, both, the higher water temperature, causing a reduction in solubility of CO_2, and a higher atmospheric CO_2 concentration, lead in combination to a slight increase in dissolved inorganic carbon in the beginning and a neutral signal towards the end of the century.

In the presented study the mobilization of terrigenous organic material is exclusively controlled by inundation. A model that also considers the impact of precipitation, vegetation cover and slope on erosion would likely lead to an increase in erosion and thus to the import of organic matter to the river (McClain and Elsenbeer, 2001) in the first years after deforestation. However, this additional influx of carbon would only be temporal, since the soil and litter carbon pools would be eroded after some years (McClain and Elsenbeer, 2001). Thus, we assume that for the investigation of the long-term dynamics of carbon pools and fluxes, such erosion effects are only of minor importance.

4.4 Consequences of the changed carbon export from the basin

The deforestation of rainforest will not only affect processes within the rainforest, but also processes in the adjacent Atlantic Ocean. Currently, the annual export of about 6300 km^3 of freshwater is accompanied by 40×10^{12} g of organic carbon to the Atlantic Ocean (Gaillardet et al., 1997; Moreira-Turcq et al., 2003). The present study shows that deforestation leads to a reduction in the exported organic carbon to the ocean by approximately 40 %. In the NatVeg scenario the proportion of exported organic carbon to the ocean makes up about 0.8–0.9 % of the net primary productions (NPP), whereas in the heavily deforested BAU scenario this proportion is reduced to about 0.5–0.6 %. The reduction in the ratio of exported carbon to NPP by deforestation indicates a less pronounced future sink, since the organic carbon is directly extracted from the forest and additionally indirectly from the ocean. The import of organic material to the ocean positively impacts the respiration and production of the Atlantic Ocean off the coast of South America (Körtzinger, 2003; Cooley and Yager, 2006; Cooley et al., 2007; Subramaniam et al., 2008). A reduction of the import might therefore reduce the productivity in the coast-near ocean. Besides the reduced organic carbon, there might be an ele-

ESDD
6, 2101–2136, 2015

vated amount of nutrients, which are only marginally taken up within the river and by the former intact adjacent forests. The imports of both, less organic carbon and more nutrients, might induce changes in oceanic heterotrophy and primary production.

5 Conclusions

Deforestation is associated with a decrease in terrestrial biomass and an increase in CO_2 emissions, which leads to a reduction in the terrestrial sequestration potential (Houghton et al., 2000; Potter et al., 2009). On top, our results show that deforestation will lead to a significant decrease of exported terrigenous organic carbon, leading to a reduction in riverine organic carbon. The climate change effects, such as increased atmospheric CO_2 concentration, lead to an increase in riverine inorganic carbon. Climate change alone will lead to an increase in riverine organic carbon of about 10 %, almost no changes in export to the Atlantic Ocean, and a drastic increase in outgassed carbon of about 40 % (Langerwisch et al., 2015). In combination with deforestation riverine organic carbon will decrease by about 20 %, export of organic carbon to the ocean will decrease by about 40 %, while outgassed carbon slightly increases.

These changes in the hydrological regimes and the fluvial carbon pools might add to the pressures that are being encountered in the Amazon ecosystems (Asner et al., 2006; Asner and Alencar, 2010) and its consequences on ecosystem stability (Brown and Lugo, 1990; Foley et al., 2002; von Randow et al., 2004). For instance, fish play a key role in seed dispersal in along the Amazon, and if floodplains turn less productive ground for juvenile fish, these changes might affect even vegetation composition (Horn et al., 2011). We therefore strongly advocate the combined terrestrial and fluvial perspective of our approach, and its ability to address both climate and land use change.

ESDD
6, 2101–2136, 2015

The Supplement related to this article is available online at doi:10.5194/esdd-6-2101-2015-supplement.

Author contributions. Model development: F. Langerwisch, B. Tietjen, WC. Data analysis: F. Langerwisch, A. Rammig, K. Thonicke. Drafting the article: F. Langerwisch, A. Walz, B. Tietjen, A. Rammig, K. Thonicke.

Acknowledgements. We thank "Pakt für Forschung der Leibniz-Gemeinschaft" for funding the TRACES project for F. Langerwisch. A. Rammig was funded by FP7 AMAZALERT (Project ID 282664) and Helmholtz Alliance "Remote Sensing and Earth System Dynamics". We also thank Susanne Rolinski and Dieter Gerten for discussing the hydrological aspects. We thank Alice Boit for fruitful comments on the manuscript. Additionally we thank our LPJmL and ECOSTAB colleagues at PIK for helpful comments on the design of the study and the manuscript.

References

Anderson, J. T., Nuttle, T., Saldaña Rojas, J. S., Pendergast, T. H., and Flecker, A. S.: Extremely long-distance seed dispersal by an overfished Amazonian frugivore, P. Roy. Soc. B, 278, 3329–3335, doi:10.1098/rspb.2011.0155, 2011.

Asner, G. P. and Alencar, A.: Drought impacts on the Amazon forest: the remote sensing perspective, New Phytol., 187, 569–578, doi:10.1111/j.1469-8137.2010.03310.x, 2010.

Asner, G. P., Broadbent, E. N., Oliveira, P. J. C., Keller, M., Knapp, D. E., and Silva, J. N. M.: Condition and fate of logged forests in the Brazilian Amazon, P. Natl. Acad. Sci. USA, 103, 12947–12950, 2006.

Bauer, D. F.: Constructing confidence sets using rank statistics, J. Am. Stat. Assoc., 67, 687–690 1972.

Bernardes, M. C., Martinelli, L. A., Krusche, A. V., Gudeman, J., Moreira, M., Victoria, R. L., Ometto, J. P. H. B., Ballester, M. V. R., Aufdenkampe, A. K., Richey, J. E., and Hedges, J. I.: Riverine organic matter composition as a function of land use changes, Southwest Amazon, Ecol. Appl., 14, S263–S279, doi:10.1890/01-6028, 2004.

ESDD
6, 2101–2136, 2015

Biemans, H., Hutjes, R. W. A., Kabat, P., Strengers, B. J., Gerten, D., and Rost, S.: Effects of precipitation uncertainty on discharge calculations for main river basins, J. Hydrometeorol., 10, 1011–1025, doi:10.1175/2008jhm1067.1, 2009.
Bondeau, A., Smith, P. C., Zaehle, S., Schaphoff, S., Lucht, W., Cramer, W., Gerten, D., Lotze-Campen, H., Müller, C., Reichstein, M., and Smith, B.: Modelling the role of agriculture for the 20th century global terrestrial carbon balance, Global Change Biol., 13, 679–706, doi:10.1111/j.1365-2486.2006.01305.x, 2007.
Brown, S. and Lugo, A. E.: Tropical secondary forests, J. Trop. Ecol., 6, 1–32, 1990.
Collatz, G. J., Ribas-Carbo, M., and Berry, J. A.: Coupled photosynthesis-stomatal conductance model for leaves of C4 plants, Funct. Plant Biol., 19, 519–538, doi:10.1071/PP9920519, 1992.
Cooley, S. R. and Yager, P. L.: Physical and biological contributions to the western tropical North Atlantic Ocean carbon sink formed by the Amazon River plume, J. Geophys. Res.-Oceans, 111, C08018, doi:10.1029/2005JC002954, 2006.
Cooley, S. R., Coles, V. J., Subramaniam, A., and Yager, P. L.: Seasonal variations in the Amazon plume-related atmospheric carbon sink, Global Biogeochem. Cy., 21, GB3014, doi:10.1029/2006GB002831, 2007.
Costa, M. H., Botta, A., and Cardille, J. A.: Effects of large-scale changes in land cover on the discharge of the Tocantins River, Southeastern Amazonia, J. Hydrol., 283, 206–217, doi:10.1016/S0022-1694(03)00267-1, 2003.
Costa, M. H., Yanagi, S. N. M., Souza, P., Ribeiro, A., and Rocha, E. J. P.: Climate change in Amazonia caused by soybean cropland expansion, as compared to caused by pastureland expansion, Geophys. Res. Lett., 34, L07706, doi:10.1029/2007GL029271, 2007.
Cramer, W., Bondeau, A., Woodward, F. I., Prentice, I. C., Betts, R. A., Brovkin, V., Cox, P. M., Fisher, V., Foley, J. A., Friend, A. D., Kucharik, C., Lomas, M. R., Ramankutty, N., Sitch, S., Smith, B., White, A., and Young-Molling, C.: Global response of terrestrial ecosystem structure and function to CO_2 and climate change: results from six dynamic global vegetation models, Global Change Biol., 7, 357–373, 2001.
Eva, H. D., Belward, A. S., De Miranda, E. E., Di Bella, C. M., Gond, V., Huber, O., Jones, S., Sgrenzaroli, M., and Fritz, S.: A land cover map of South America, Global Change Biol., 10, 731–744, 2004.

ESDD
6, 2101–2136, 2015

Deforestation in Amazonia impacts riverine carbon dynamics

F. Langerwisch et al.

Title Page
Abstract Introduction
Conclusions References
Tables Figures
◂ ▸
Back Close
Full Screen / Esc
Printer-friendly Version
Interactive Discussion

Fader, M., Rost, S., Müller, C., Bondeau, A., and Gerten, D.: Virtual water content of temperate cereals and maize: present and potential future patterns, J. Hydrol., 384, 218–231, doi:10.1016/j.jhydrol.2009.12.011, 2010.
Farquhar, G. D., van Caemmerer, S., and Berry, J. A.: A biochemical model of photosynthetic CO_2 assimilation in leaves of C3 species, Planta, 149, 78–90, 1980.
Foley, J. A., Botta, A., Coe, M. T., and Costa, M. H.: El Niño–Southern Oscillation and the climate, ecosystems and rivers of Amazonia, Global Biogeochem. Cy., 16, 79/1–79/17, doi:10.1029/2002GB001872, 2002.
Foley, J. A., Asner, G. P., Costa, M. H., Coe, M. T., DeFries, R., Gibbs, H. K., Howard, E. A., Olson, S., Patz, J., Ramankutty, N., and Snyder, P.: Amazonia revealed: forest degradation and loss of ecosystem goods and services in the Amazon Basin, Front. Ecol. Environ., 5, 25–32, doi:10.1890/1540-9295(2007)5[25:ARFDAL]2.0.CO;2, 2007.
Gaillardet, J., Dupré, B., Allègre, C. J., and Négrel, P.: Chemical and physical denudation in the Amazon River basin, Chem. Geol., 142, 141–173, 1997.
Gerten, D., Schaphoff, S., Haberlandt, U., Lucht, W., and Sitch, S.: Terrestrial vegetation and water balance – hydrological evaluation of a dynamic global vegetation model, J. Hydrol., 286, 249–270, doi:10.1016/j.jhydrol.2003.09.029, 2004.
Gerten, D., Rost, S., von Bloh, W., and Lucht, W.: Causes of change in 20th century global river discharge, Geophys. Res. Lett., 35, L20405, doi:10.1029/2008gl035258, 2008.
Godar, J., Gardner, T. A., Tizado, E. J., and Pacheco, P.: Actor-specific contributions to the deforestation slowdown in the Brazilian Amazon, P. Natl. Acad. Sci. USA, 111, 15591–15596, doi:10.1073/pnas.1322825111, 2014.
Gordon, W. S., Famiglietti, J. S., Fowler, N. L., Kittel, T. G. F., and Hibbard, K. A.: Validation of simulated runoff from six terrestrial ecosystem models: results from VEMAP, Ecol. Appl., 14, 527–545, doi:10.1890/02-5287, 2004.
Goulding, M., Barthem, R., and Ferreira, E.: The Smithsonian Atlas of the Amazon, Smithsonian, Washington, London, 2003.
Hamilton, S. K.: Biogeochemical implications of climate change for tropical rivers and floodplains, Hydrobiologia, 657, 19–35, doi:10.1007/s10750-009-0086-1, 2010.
Hedges, J. I., Mayorga, E., Tsamakis, E., McClain, M. E., Aufdenkampe, A., Quay, P., Richey, J. E., Benner, R., Opsahl, S., Black, B., Pimentel, T., Quintanilla, J., and Maurice, L.: Organic matter in Bolivian tributaries of the Amazon River: a comparison to the lower mainstream, Limnol. Oceanogr., 45, 1449–1466, 2000.

ESDD
6, 2101–2136, 2015
Deforestation in Amazonia impacts riverine carbon dynamics
F. Langerwisch et al.

Hoorn, C., Wesselingh, F. P., ter Steege, H., Bermudez, M. A., Mora, A., Sevink, J., Sanmartin, I., Sanchez-Meseguer, A., Anderson, C. L., Figueiredo, J. P., Jaramillo, C., Riff, D., Negri, F. R., Hooghiemstra, H., Lundberg, J., Stadler, T., Sarkinen, T., and Antonelli, A.: Amazonia through time: andean uplift, climate change, landscape evolution, and biodiversity, Science, 330, 927–931, doi:10.1126/science.1194585, 2010.

Horn, M. H., Correa, S. B., Parolin, P., Pollux, B. J. A., Anderson, J. T., Lucas, C., Widmann, P., Tjiu, A., Galetti, M., and Goulding, M.: Seed dispersal by fishes in tropical and temperate fresh waters: the growing evidence, Acta Oecol., 37, 561–577, doi:10.1016/j.actao.2011.06.004, 2011.

Houghton, R. A., Skole, D. L., Nobre, C. A., Hackler, J. L., Lawrence, K. T., and Chomentowski, W. H.: Annual fluxes or carbon from deforestation and regrowth in the Brazilian Amazon, Nature, 403, 301–304, 2000.

INPE: Projeto PRODES: Monitoramento da floresta Amazônica Brasileira por satélite, available at: http://www.obt.inpe.br/prodes/index.php (last access: 28 April 2015), 2013.

Irmler, U.: Litterfall and nitrogen turnover in an Amazonian blackwater inundation forest, Plant Soil, 67, 355–358, 1982.

Johnson, M. S., Lehmann, J., Selva, E. C., Abdo, M., Riha, S., and Couto, E. G.: Organic carbon fluxes within and streamwater exports from headwater catchments in the southern Amazon, Hydrol. Process., 20, 2599–2614, 2006.

Junk, W. J.: The Central Amazon Floodplain – Ecology of a Pulsing System, Springer, Berlin, 1997.

Junk, W. J. and Wantzen, K. M.: The flood pulse concept: new aspects, approaches and applications – an update, in: Proceedings of the Second International Symposium on the Management of large Rivers for Fisheries, edited by: Welcomme, R. L. and Petr, T., Food and Agriculture Organization and Mekong River Commission, FAO Regional Office for Asia and the Pacific, Bangkok, 117–140, 2004.

Jupp, T. E., Cox, P. M., Rammig, A., Thonicke, K., Lucht, W., and Cramer, W.: Development of probability density functions for future South American rainfall, New Phytol., 187, 682–693, doi:10.1111/j.1469-8137.2010.03368.x, 2010.

Keller, M., Bustamante, M., Gash, J., and Silva Dias, P. (Eds.): Amazonia and Global Change, American Geophysical Union, Washington, D.C., 2009.

Körtzinger, A.: A significant CO_2 sink in the tropical Atlantic Ocean associated with the Amazon River plume, Geophys. Res. Lett., 30, 2287, doi:10.1029/2003GL018841, 2003.

Langerwisch, F., Rost, S., Gerten, D., Poulter, B., Rammig, A., and Cramer, W.: Potential effects of climate change on inundation patterns in the Amazon Basin, Hydrol. Earth Syst. Sci., 17, 2247–2262, doi:10.5194/hess-17-2247-2013, 2013.

Langerwisch, F., Walz, A., Rammig, A., Tietjen, B., Thonicke, K., and Cramer, W.: Climate change increases riverine carbon outgassing while export to the ocean remains uncertain, Earth Syst. Dynam. Discuss., 6, 1445–1497, doi:10.5194/esdd-6-1445-2015, 2015.

Lawrence, D. and Vandecar, K.: Effects of tropical deforestation on climate and agriculture, Nat. Clim. Change, 5, 27–36, doi:10.1038/nclimate2430, 2014.

Malhi, Y., Wood, D., Baker, T. R., Wright, J., Phillips, O. L., Cochrane, T., Meir, P., Chave, J., Almeida, S., Arroyo, L., Higuchi, N., Killeen, T. J., Laurance, S. G., Laurance, W. F., Lewis, S. L., Monteagudo, A., Neill, D. A., Vargas, P. N., Pitman, N. C. A., Quesada, C. A., Salomão, R., Silva, J. N. M., Lezama, A. T., Terborgh, J., Martínez, R. V., and Vinceti, B.: The regional variation of aboveground live biomass in old-growth Amazonian forests, Global Change Biol., 12, 1107–1138, 2006.

Malhi, Y., Roberts, J. T., Betts, R. A., Killeen, T. J., Li, W., and Nobre, C. A.: Climate change, deforestation, and the fate of the Amazon, Science, 319, 169–172, 2008.

Mayorga, E., Aufdenkampe, A. K., Masiello, C. A., Krusche, A. V., Hedges, J. I., Quay, P. D., Richey, J. E., and Brown, T. A.: Young organic matter as a source of carbon dioxide outgassing from Amazonian rivers, Nature, 436, 538–541, doi:10.1038/nature03880, 2005.

McClain, M. E. and Elsenbeer, H.: Terrestrial inputs to Amazon streams and internal biogeochemical processing, in: The Biogeochemistry of the Amazon Basin, edited by: McClain, M. E., Victoria, R. L., and Richey, J. E., Oxford University Press, New York, 185–208, 2001.

Melack, J. M. and Forsberg, B.: Biogeochemistry of Amazon floodplain lakes and associated wetlands, in: The Biogeochemistry of the Amazon Basin and its Role in a Changing World, edited by: McClain, M. E., Victoria, R. L., and Richey, J. E., Oxford University Press, 235–276, 2001.

Moreira-Turcq, P., Seyler, P., Guyot, J. L., and Etcheber, H.: Exportation of organic carbon from the Amazon River and its main tributaries, Hydrol. Process., 17, 1329–1344, doi:10.1002/hyp.1287, 2003.

Nakićenović, N., Davidson, O., Davis, G., Grübler, A., Kram, T., Lebre La Rovere, E., Metz, B., Morita, T., Pepper, W., Pitcher, H., Sankovski, A., Shukla, P., Swart, R., and Dadi, Z.: IPCC

ESDD
6, 2101–2136, 2015

Deforestation in Amazonia impacts riverine carbon dynamics

F. Langerwisch et al.

Special report on emission scenarios, available at: https://www.ipcc.ch/pdf/special-reports/spm/sres-en.pdf (last access: 8 November 2011), 2000.
Nobre, A. D.: The Future Climate of Amazonia: Scientific Assessment Report, INPA and ARA, São José dos Campos, Brazil, available from: http://www.ccst.inpe.br/wp-content/uploads/2014/11/The_Future_Climate_of_Amazonia_Report.pdf (last access: 31 August 2015), 2014.
Potter, C., Klooster, S., and Genovese, V.: Carbon emissions from deforestation in the Brazilian Amazon Region, Biogeosciences, 6, 2369–2381, doi:10.5194/bg-6-2369-2009, 2009.
Randall, D. A., Wood, R. A., Bony, S., Colman, R., Fichefet, T., Fyfe, J., Kattsov, V., Pitman, A., Shukla, J., Srinivasan, J., Stouffer, R. J., Sumi, A., and Taylor, K. E.: Climate models and their evaluation, in: Climate Change 2007: The Physical Science Basis, Contribution of Working Group I to the Fourth Assessment Report of the Intergovernmental Panel on Climate Change, edited by: Solomon, S., Qin, D., Manning, M., Chen, Z., Marquis, M., Averyt, K. B., Tignor, M., and Miller, H. L., Cambridge University Press, 2007.
Richey, J. E., Melack, J. M., Aufdenkampe, A. K., Ballester, V. M., and Hess, L. L.: Outgassing from Amazonian rivers and wetlands as a large tropical source of atmospheric CO_2, Nature, 416, 617–620, doi:10.1038/416617a, 2002.
Rost, S., Gerten, D., Bondeau, A., Lucht, W., Rohwer, J., and Schaphoff, S.: Agricultural green and blue water consumption and its influence on the global water system, Water Resour. Res., 44, W09405, doi:10.1029/2007wr006331, 2008.
Salimon, C. I., Davidson, E. A., Victoria, R. L., and Melo, A. W. F.: CO_2 flux from soil in pastures and forests in southwestern Amazonia, Global Change Biol., 10, 833–843, 2004.
Sitch, S., Smith, B., Prentice, I. C., Arneth, A., Bondeau, A., Cramer, W., Kaplan, J. O., Levis, S., Lucht, W., Sykes, M. T., Thonicke, K., and Venevsky, S.: Evaluation of ecosystem dynamics, plant geography and terrestrial carbon cycling in the LPJ dynamic global vegetation model, Global Change Biol., 9, 161–185, doi:10.1046/j.1365-2486.2003.00569.x, 2003.
Soares-Filho, B. S., Nepstad, D. C., Curran, L. M., Cerqueira, G. C., Garcia, R. A., Ramos, C. A., Voll, E., McDonald, A., Lefebvre, P., and Schlesinger, P.: Modelling conservation in the Amazon basin, Nature, 440, 520–523, 2006.
Spracklen, D. V., Arnold, S. R., and Taylor, C. M.: Observations of increased tropical rainfall preceded by air passage over forests, Nature, 489, 282–285, doi:10.1038/nature11390, 2012.
Subramaniam, A., Yager, P. L., Carpenter, E. J., Mahaffey, C., Bjorkman, K., Cooley, S., Kustka, A. B., Montoya, J. P., Sanudo-Wilhelmy, S. A., Shipe, R., and Capone, D. G.: Amazon

ESDD
6, 2101–2136, 2015

River enhances diazotrophy and carbon sequestration in the tropical North Atlantic Ocean, P. Natl. Acad. Sci. USA, 105, 10460–10465, doi:10.1073/pnas.0710279105, 2008.

Thonicke, K., Spessa, A., Prentice, I. C., Harrison, S. P., Dong, L., and Carmona-Moreno, C.: The influence of vegetation, fire spread and fire behaviour on biomass burning and trace gas emissions: results from a process-based model, Biogeosciences, 7, 1991–2011, doi:10.5194/bg-7-1991-2010, 2010.

von Randow, C., Manzi, A. O., Kruijt, B., de Oliveira, P. J., Zanchi, F. B., Silva, R. L., Hodnett, M. G., Gash, J. H. C., Elbers, J. A., Waterloo, M. J., Cardoso, F. L., and Kabat, P.: Comparative measurements and seasonal variations in energy and carbon exchange over forest and pasture in South West Amazonia, Theor. Appl. Climatol., 78, 5–26, doi:10.1007/s00704-004-0041-z, 2004.

Wagner, W., Scipal, K., Pathe, C., Gerten, D., Lucht, W., and Rudolf, B.: Evaluation of the agreement between the first global remotely sensed soil moisture data with model and precipitation data, J. Geophys. Res., 108, 4611, doi:10.1029/2003JD003663, 2003.

Waterloo, M. J., Oliveira, S. M., Drucker, D. P., Nobre, A. D., Cuartas, L. A., Hodnett, M. G., Langedijk, I., Jans, W. W. P., Tomasella, J., de Araújo, A. C., Pimentel, T. P., and Estrada, J. C. M.: Export of organic carbon in run-off from an Amazonian rainforest blackwater catchment, Hydrol. Process., 20, 2581–2597, 2006.

Worbes, M.: The forest ecosystem of the floodplains, in: The Central Amazon Floodplain, edited by: Junk, W. J., Springer, Berlin, Germany, 223–265, 1997.

ESDD
6, 2101–2136, 2015

Table 1. Location and characteristics of the three sub-regions.

	North-West corner	South-East corner	area [10^3 km^2]	inundation length	inundated area	land use intensity
R1	0.5° S/78.5° W	7.0° S/72° W	523.03	1 month longer	larger	low
R2	1.0° S/70.0° W	5.0° S/52° W	891.32	±1/2 month shift	heterogeneous	medium
R3	4.5° S/58.0° W	11.0° S/52° W	523.03	1/2 month shorter	smaller	high

Regions are depicted in Fig. 2. Changes in inundation discussed in Langerwisch et al. (2013).

ESDD
6, 2101–2136, 2015

Table 2. Basin-wide (B) and region wise (R1–R3) amount of carbon in POC and DOC, outgassed carbon and IC [10^{12} g month^{-1}] averaged over 30 years and five climate models.

	$NatVeg_{ref}$	$NatVeg_{fut}$	$GOV_{fut\ A1B}$	$BAU_{fut\ A1B}$	$GOV_{fut\ A2}$	$BAU_{fut\ A2}$	$GOV_{fut\ B1}$	$BAU_{fut\ B1}$
POC								
B	1.64 ± 0.06	1.76 ± 0.51	1.52 ± 0.43	1.28 ± 0.35	1.63 ± 0.41	1.39 ± 0.34	1.55 ± 0.31	1.30 ± 0.24
R1	0.16 ± 0.01	0.22 ± 0.05	0.20 ± 0.05	0.20 ± 0.05	0.21 ± 0.05	0.21 ± 0.05	0.18 ± 0.02	0.18 ± 0.02
R2	0.42 ± 0.01	0.43 ± 0.15	0.37 ± 0.12	0.30 ± 0.09	0.40 ± 0.13	0.33 ± 0.10	0.38 ± 0.09	0.31 ± 0.07
R3	0.15 ± 0.01	0.14 ± 0.05	0.11 ± 0.04	0.07 ± 0.03	0.12 ± 0.04	0.08 ± 0.02	0.12 ± 0.03	0.08 ± 0.02
DOC								
B	3.41 ± 0.13	3.58 ± 1.05	3.07 ± 0.87	2.59 ± 0.71	3.29 ± 0.84	2.77 ± 0.69	3.15 ± 0.63	2.64 ± 0.48
R1	0.34 ± 0.02	0.46 ± 0.11	0.43 ± 0.10	0.42 ± 0.10	0.45 ± 0.10	0.44 ± 0.10	0.39 ± 0.05	0.38 ± 0.05
R2	0.93 ± 0.03	0.91 ± 0.32	0.77 ± 0.26	0.64 ± 0.20	0.84 ± 0.27	0.69 ± 0.21	0.81 ± 0.20	0.66 ± 0.15
R3	0.34 ± 0.02	0.30 ± 0.11	0.24 ± 0.09	0.16 ± 0.06	0.26 ± 0.08	0.17 ± 0.05	0.27 ± 0.07	0.17 ± 0.04
Outgassed carbon								
B	11.82 ± 0.41	16.63 ± 4.14	14.30 ± 3.44	12.05 ± 2.76	15.75 ± 3.43	13.24 ± 2.80	13.37 ± 2.20	11.15 ± 1.68
R1	1.15 ± 0.06	2.05 ± 0.38	1.93 ± 0.35	1.91 ± 0.35	2.10 ± 0.35	2.08 ± 0.35	1.61 ± 0.13	1.60 ± 0.14
R2	2.52 ± 0.08	3.36 ± 0.99	2.81 ± 0.78	2.37 ± 0.6	3.09 ± 0.85	2.59 ± 0.66	2.66 ± 0.56	2.22 ± 0.43
R3	0.99 ± 0.04	1.12 ± 0.42	0.91 ± 0.34	0.55 ± 0.20	1.03 ± 0.32	0.62 ± 0.18	0.94 ± 0.26	0.56 ± 0.14
IC								
B	0.227 ± 0.003	0.457 ± 0.119	0.457 ± 0.120	0.456 ± 0.121	0.523 ± 0.137	0.522 ± 0.138	0.365 ± 0.063	0.364 ± 0.064
R1	0.005 ± 0.001	0.016 ± 0.003	0.013 ± 0.003	0.013 ± 0.003	0.015 ± 0.004	0.015 ± 0.004	0.009 ± 0.001	0.009 ± 0.001
R2	0.153 ± 0.002	0.308 ± 0.081	0.308 ± 0.082	0.307 ± 0.083	0.351 ± 0.094	0.350 ± 0.096	0.245 ± 0.044	0.244 ± 0.044
R3	0.006 ± 0.0001	0.011 ± 0.003	0.011 ± 0.003	0.011 ± 0.003	0.013 ± 0.003	0.013 ± 0.003	0.009 ± 0.001	0.009 ± 0.001

"ref" refers to mean amounts during reference period 1971–2000. "fut" refers to mean amounts during future period 2070–2099. Values given are the mean ± standard deviation of the five climate models.

ESDD
6, 2101–2136, 2015

Deforestation in Amazonia impacts riverine carbon dynamics

F. Langerwisch et al.

Table 3. Proportion [%] of area dominated by climate or land use change impacts.

	Climate change dominated			Land use change dominated			Balanced		
	A1B	A2	B1	A1B	A2	B1	A1B	A2	B1
POC									
GOV	29.9	29.9	27.9	20.8	20.7	22.7	0.15	0.31	0.26
BAU	21.5	22.2	20.4	29.2	28.6	30.4	0.10	0.05	0.05
IC									
GOV	50.8	50.8	50.8	0.0	0.0	0.0	0.00	0.00	0.00
BAU	50.8	50.8	50.8	0.0	0.0	0.0	0.00	0.00	0.00
Outgassed carbon									
GOV	68.8	75.8	66.8	28.6	21.8	30.4	0.21	0.00	0.41
BAU	51.1	55.6	49.0	46.4	42.0	48.5	0.05	0.05	0.10

If both impacts compensate each other the cell is balanced.

ESDD
6, 2101–2136, 2015

Deforestation in Amazonia impacts riverine carbon dynamics

F. Langerwisch et al.

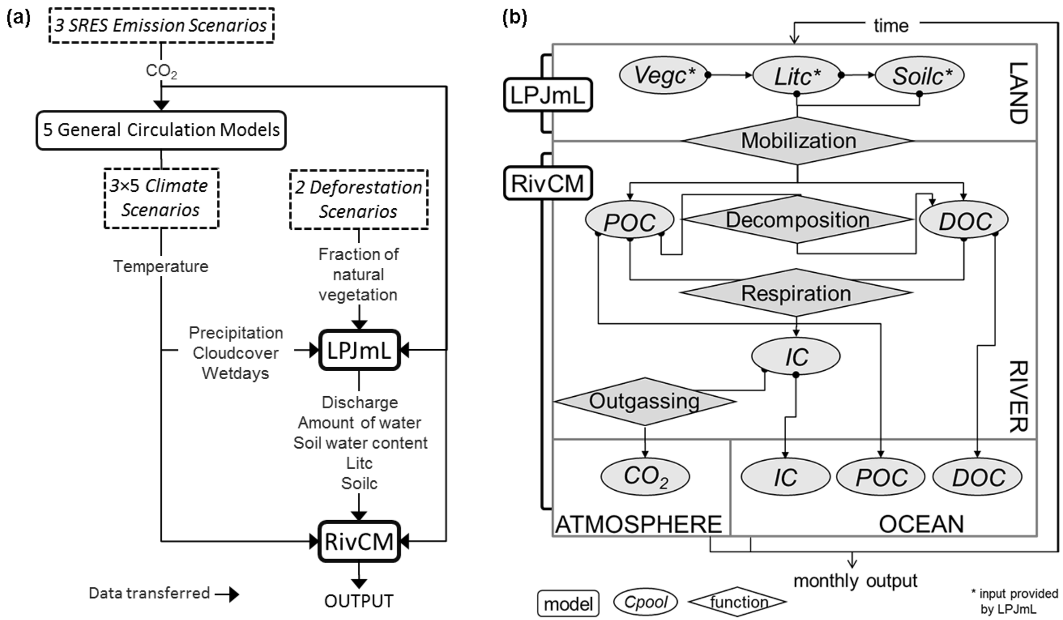

Figure 1. Overview of the general transfer of data between scenarios and models **(a)** and the detailed calculation of carbon fluxes within and between LPJmL and RivCM.

ESDD
6, 2101–2136, 2015

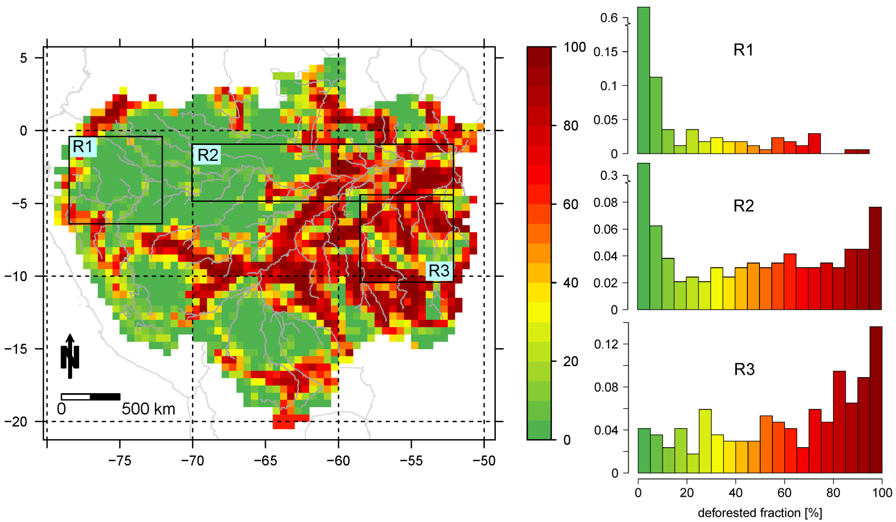

Figure 2. Fraction of deforested area per cell [%] in 2050. Data are based on Soares-Filho et al. (2006). The three sub-regions discussed in the main text are highlighted in the map. The histograms (right panels) show the proportion of 20 deforestation classes (0–5 % deforested to 95–100 % deforested) in each sub-region.

ESDD
6, 2101–2136, 2015

Deforestation in Amazonia impacts riverine carbon dynamics

F. Langerwisch et al.

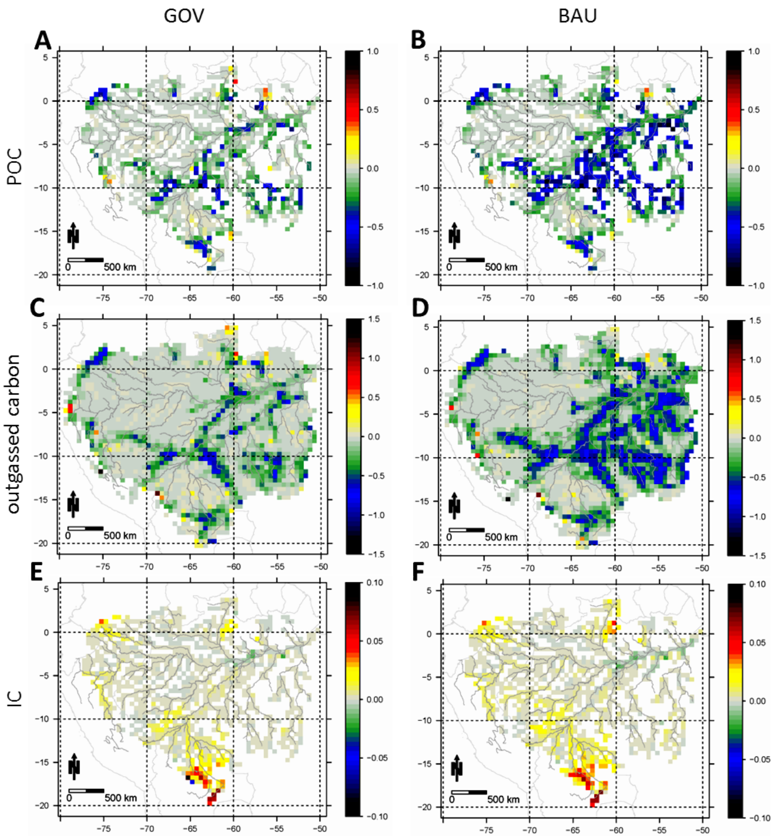

Figure 3. Change in carbon caused by deforestation. Climate model mean (E_{Defor}) of the change of particulate organic carbon POC **(a, b)**, outgassed carbon **(c, d)** and inorganic carbon IC **(e, f)**. Results of the SRES emission scenario A1B are averaged over five climate models. Positive values (yellow and red) indicate a gain and negative values (green and blue) indicate a loss in carbon caused by deforestation (GOV and BAU).

ESDD
6, 2101–2136, 2015

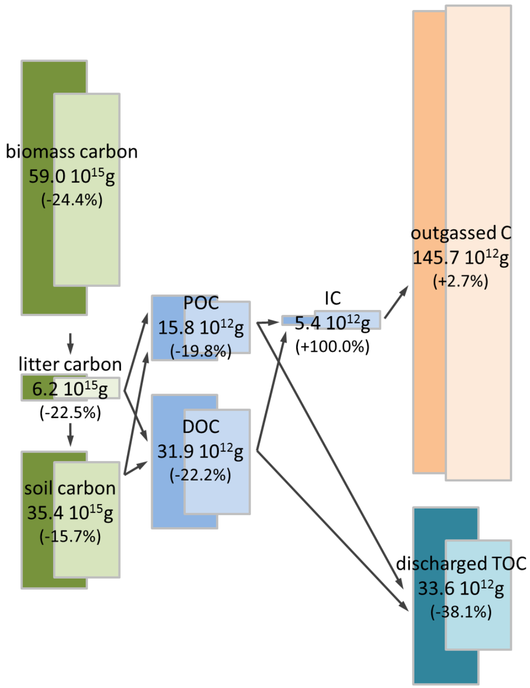

Figure 4. Averaged annual amounts and change in the basin carbon budget due to climate change and deforestation. Dark boxes indicate the amount of carbon during the reference period, light boxes during the future period (average over all SRES scenarios and GCMs). Amount is given for future period with relative change compared to reference. Arrows indicate the direction of carbon transfer.

ESDD
6, 2101–2136, 2015

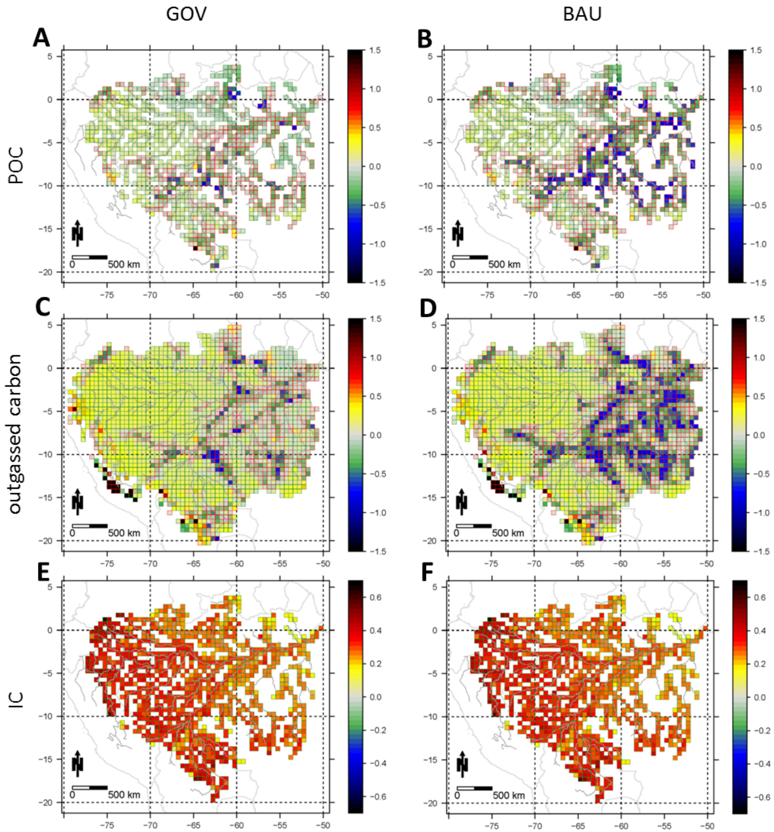

Figure 5. Change in carbon caused by deforestation and climate change. Climate model mean ($E_{CCDefor}$) of the change of particulate organic carbon POC **(a, b)**, outgassed carbon **(c, d)** and inorganic carbon IC **(e, f)**. In cells with a green border change are predominantly caused by climate change, in cells with a red border changes are predominantly caused by deforestation. For further details see Fig. 3.

ESDD
6, 2101–2136, 2015

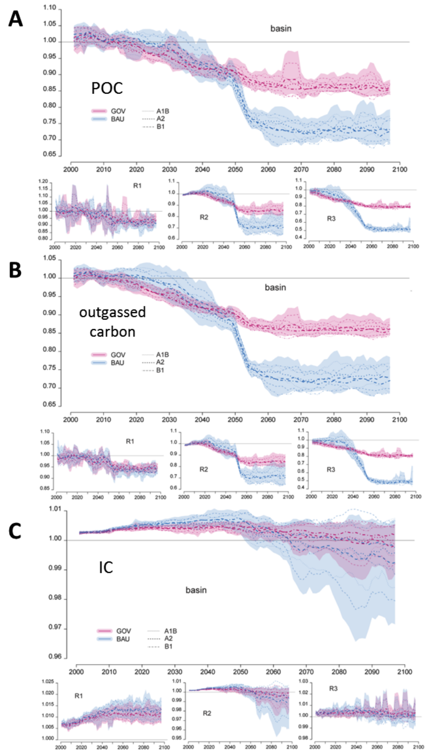

Figure 6. Temporal change in particulate organic carbon due to land use change. Quotient of annual sum of carbon in the deforestation scenario (GOV or BAU) and in the NatVeg scenario for the whole basin and the three sub-regions (R1–R3) as 5 year-mean for GOV (red) and BAU (blue). The shaded areas indicate the full range of values of all five climate models. Bold lines represent the 5 year-mean and thin lines represent mean ±1.0 standard deviation of the five climate models. Values larger 1.0 indicate an increase in carbon in the deforestation scenario, compared to the NatVeg scenario, values smaller than 1.0 indicate a decrease (no change is indicated by the horizontal line).

ESDD
6, 2101–2136, 2015